Microstructural Aspects of Superplasticity

JEFF W. EDINGTON

This short review summarizes the contribution of microstructural studies to the present understanding of the deformation mechanisms operating during superplastic deformation. A background summary is included that describes the major features of superplasticity, the relevant deformation theories, and the requirements for successful microstructural studies. However, most of the paper is concentrated on a discussion of the microstructural evidence in the literature on two types of material. The first is a representative group of modern commercial nickel, aluminum, and magnesium alloys. The second is the Zn-Al eutectoid, a member of the well characterized "classical" group of superplastic materials based upon eutectic or eutectoid compositions. The importance of dislocation motion at maximum m is emphasized, both as an accommodation mechanism for grain boundary sliding and directly in response to the applied stress. However, it is shown that, in IN100 and Supral 150, other processes occur simultaneously, including recrystallization and diffusion.

I. INTRODUCTION

THE most useful characteristic of superplastic materials is their ability to deform at low applied stresses to exceptionally large strains (4850 pct is the maximum tensile elongation reported to date[1]). Clearly, superplastic forming is of considerable interest. Potential cost reductions are large, and considerable freedom is provided in designing complex components. Consequently, several companies have been producing superplastically formed components in aluminum, titanium, nickel, and zinc based alloys for more than five years. There are many patents describing superplastic materials and a partial listing can be found in Reference 2.

Superplasticity was first demonstrated in 1934[3] with a tensile elongation of 1950 pct in a Sn-Bi eutectic alloy. This sensational result was largely ignored for almost 30 years, but interest was stimulated in the early 1960's by the review of Russian work in the area of Underwood,[4] together with the pioneering work of Backofen and his co-workers.[5-10] Since then considerable research has been conducted on the phenomenon and the major conclusions may be summarized as follows: Firstly, there is a good understanding of the requirements for microstructure, test temperature, and strain rate for successful superplastic deformation, as well as the methods by which they may be achieved in commercial alloys. Secondly, suitable industrial forming techniques exist. Thirdly, many of the deformation mechanisms that operate during superplastic flow are known, but very few quantitative measurements of their contribution to the total strain are available. Fourthly, none of the theories is entirely consistent with all experimental observations.

The subject has been reviewed extensively including mechanical properties, metallographic and crystallographic texture changes, and operative mechanisms;[11] the principles behind development and superplasticity in commercial alloys;[2] the deformation mechanisms;[12] and the flow and fracture characteristics.[13] The objective of this paper is to review the microstructural data relevant to the identification of deformation mechanisms, with particular emphasis on work conducted since the last review in 1976.[11] As illustrations, two types of material are discussed. These are (a) several examples of the modern class of commercial alloys produced by controlled thermo-mechanical processing and (b) the classical Zn-Al alloy with the eutectoid composition. The term microstructural is defined in its broadest sense to include, not only information from conventional optical and electron optical techniques, but also from quantitative texture analysis.

JEFF W. EDINGTON is with Alcan Laboratories, Ltd., Southam Road, Banbury, Oxon OX16 7SP, United Kingdom.

This paper is based on a presentation made at the symposium "On the Mechanical, Microstructural and Fracture Processes in Superplasticity" held at the annual meeting of the AIME in Pittsburgh, PA on October 7, 1980 under the sponsorship of the Flow and Fracture Activity of the Materials Science Division of ASM.

II. SUMMARY OF THE MAJOR FEATURES OF SUPERPLASTICITY

To serve as an introduction to the main paper, it is useful to summarize the important general features of superplasticity that have been dealt with in detail in the reviews[11,12,13] listed above. These were as follows:

1. Almost all superplastic materials had a fine equiaxed grain size $\leq 10\ \mu m$. The grain size was usually stabilized by the presence of a large volume fraction (30 to 50 pct) of second phase as particles approximately equal to the matrix grain size. The grains grew only slightly (times two) during superplastic deformation, but remained essentially equiaxed so that the grain elongation was considerably less than the macroscopic specimen elongation.
2. Superplasticity was exhibited only on deformation above approximately half the melting point and over a specific range of strain rates, usually $\sim 10^{-2}$ to 10^{-4} sec^{-1}.
3. There was a sigmoidal relationship between the logarithms of stress and strain rate (see Figure 1). It was in the region of maximum slope that large elongation was obtained. Conventionally, the sigmoidal curve has been divided into three regions; superplasticity occurred in region II only.
4. The strain rate sensitivity of the flow stress has been referred to as $m = (d \ln \sigma)/(d \ln \dot{\varepsilon})$ and is a maximum near the center of region II (see Figure 1). The value of m increased with increased temperature and decreased grain size. This has important implications for superplastic forming.[4] Commonly, the value of m lay in the range of 0.3 to 0.9. A value of 1.0 corresponds to Newtonian viscous flow.
5. Neck development was opposed primarily by the high strain rate sensitivity of the flow stress. For phenomenological treatments see References 11,15, and 16.

ISSN 0360-2133/82/0511-0703$00.75/0

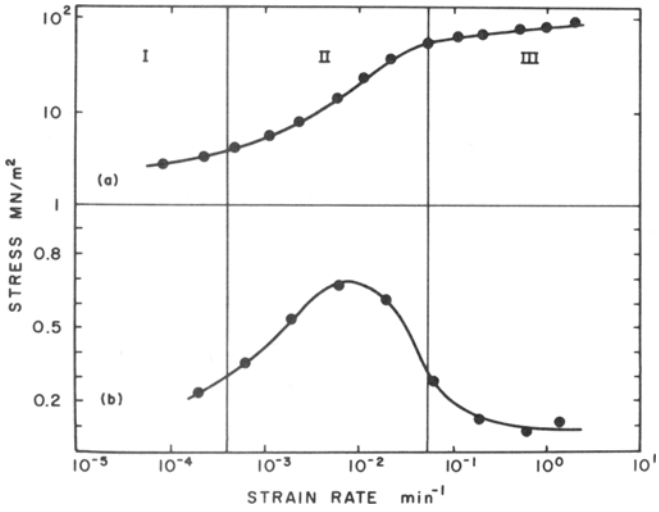

Fig. 1—The strain rate ($\dot{\varepsilon}$) dependence of (a) the flow stress (σ) and (b) the parameter $m = \delta \ln \sigma / \delta \ln \dot{\varepsilon}$ for the Mg-Al alloy, grain size 10.6 μm deformed at 350 °C. After Lee.[19]

6. The mechanical properties may be analyzed in terms of thermally activated processes, and this is discussed in detail by Langdon.[17]
7. The fracture processes frequently included cavitation.[13,18]
8. There was considerable grain boundary sliding (GBS) and reduction of texture in region II of Figure 1, but much less in region III.
9. There were weak stable texture components present after large superplastic strains. These have been interpreted in terms of slip in individual grains under the action of the applied stress. By implication it was therefore very likely to be an accommodation mechanism to relieve the high stress concentration produced by GBS.
10. There was little transmission electron microscopy evidence for dislocations in superplastically deformed material, although this could have been caused by experimental difficulties in retaining them after the end of the tensile test (see section IV).

III. SUMMARY OF PROPOSED THEORIES OF SUPERPLASTICITY

It has been clear for some time[11] that GBS played a major role in superplastic deformation, region II, of many alloys. Figure 2 shows clear evidence for GBS in a Sn5 pct Bi alloy. Note the scratch offset, arrowed, and the new grain surface S. Rotation of the grain below S has also taken place. *In situ* SEM studies[21,22,23] of the Pb-Sn eutectic material have also provided clear evidence of extensive GBS and grain motion over distances equal to many grain diameters. There were differences in detail, however. Groups of grains were reported to slide and rotate as units in two studies.[21,23] In contrast, other evidence[22] showed that most grain boundaries appeared to slide individually although all did not necessarily slide simultaneously.

For the above reasons, only those mechanisms that are based upon GBS are relevant. However, in order to maintain grain contact, extensive material transport (accommodation) is necessary. Consequently, this is generally included as part of the overall deformation mechanism.

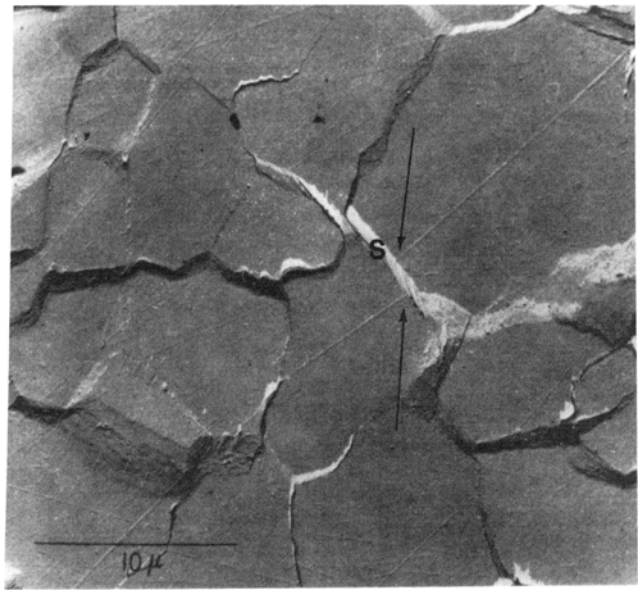

Fig. 2—An electron micrograph of a replica taken from a Sn-5 pct Bi alloy deformed to 10 pct strain ($\dot{\varepsilon} = 3.3 \times 10^{-5} \text{sec}^{-1} m = 0.4$), showing a scratch offset, arrowed, and a new grain surface S. After Alden.[20]

A. *Grain Boundary Sliding, Diffusion Accommodated Flow Rate Controlling (Figure 3)*

The theory was developed by Ashby and Verrall[24] to describe the grain switching event illustrated schematically in Figure 3. Two processes operated. Firstly, GBS occurred with material transport by grain boundary and bulk diffusion to maintain grain continuity. Secondly, dislocation creep took place but made a decreasing contribution as the strain rate was reduced in the transition between regions III and II and was insignificant at maximum m.

The characteristics of this model included the following:

1. The $\ln \sigma / \ln \dot{\varepsilon}$ curve was sigmoidal.
2. In region I and most of region II there was no large grain elongation, neither was there important dislocation motion or cell formation, but there was extensive GBS and grain rotation.
3. At the high strain rate (upper) end of region II, dislocation motion was important and contributed to both the total strain and accommodation process. There was significant but reduced GBS and grain rotation.
4. In region III dislocation creep was dominant, GBS contributed less, texture could be created, and grains elongated.
5. Activation energies were equivalent to grain boundary diffusion in regions I and II and bulk diffusion in region III.

Consequently, this theory accounted qualitatively for all points in Section II except 7 and 9. However, the input data for the equations were not available for most alloys to provide a quantitative check.

Valiev and Kaibyshev[25] have also suggested a model in which the strain rate in region II was explained in terms of local diffusion accommodation of GBS. They proposed that this approach should be modified to account for the contribution of dislocation motion but did not describe how this should be done.

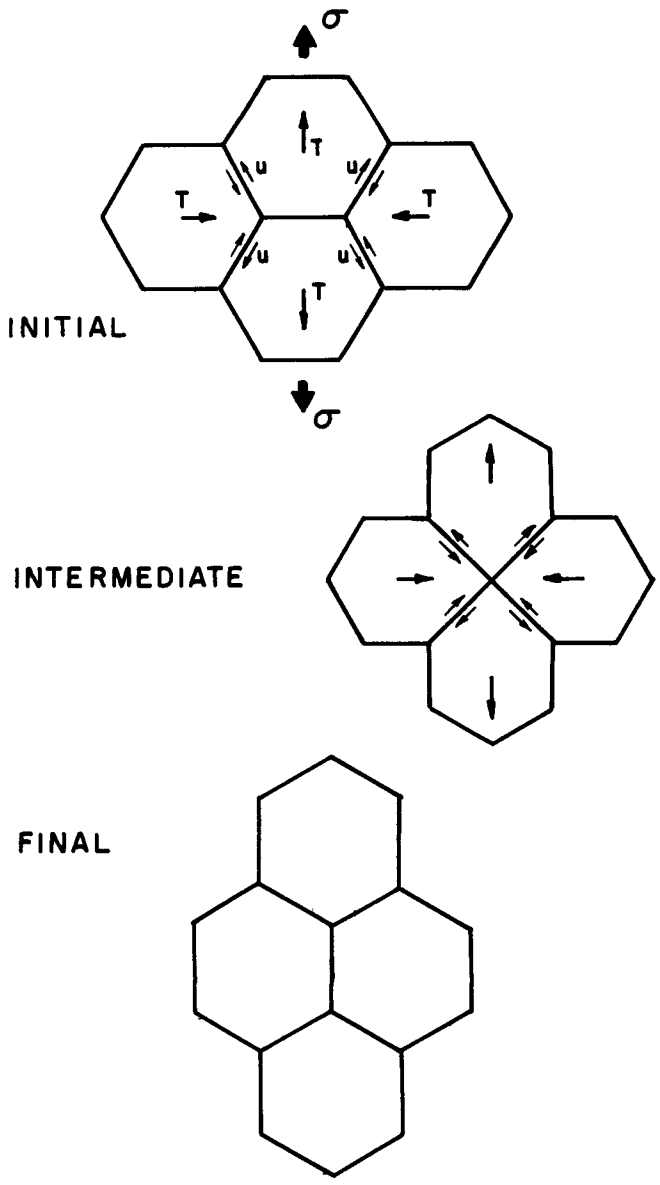

Fig. 3—A schematic illustration of the grain switching mechanism.[24]

B. *Grain Boundary Sliding, Dislocation Motion Accommodation Rate Controlling*

There have been several relatively detailed treatments of superplasticity in terms of GBS with rate-controlling accommodation at triple points by dislocation motion. These are illustrated schematically in Figures 4(a) to (c).

Ball and Hutchison[26] proposed that, in region II, groups of grains could slide as a unit until it was obstructed by an unfavorably oriented grain (see Figure 4(a)). The resultant stress concentration was released by dislocation motion in the blocking grain. These dislocations piled up until the back stress stopped the source and therefore the sliding process. Continuation of sliding required climb by the leading dislocation into and along the boundary, so that further sliding occurred at a rate governed by the kinetics of grain boundary climb of dislocations toward annihilation sites.

Mukherjee[27] has proposed a modification of this model in which the grains slid individually while dislocations were

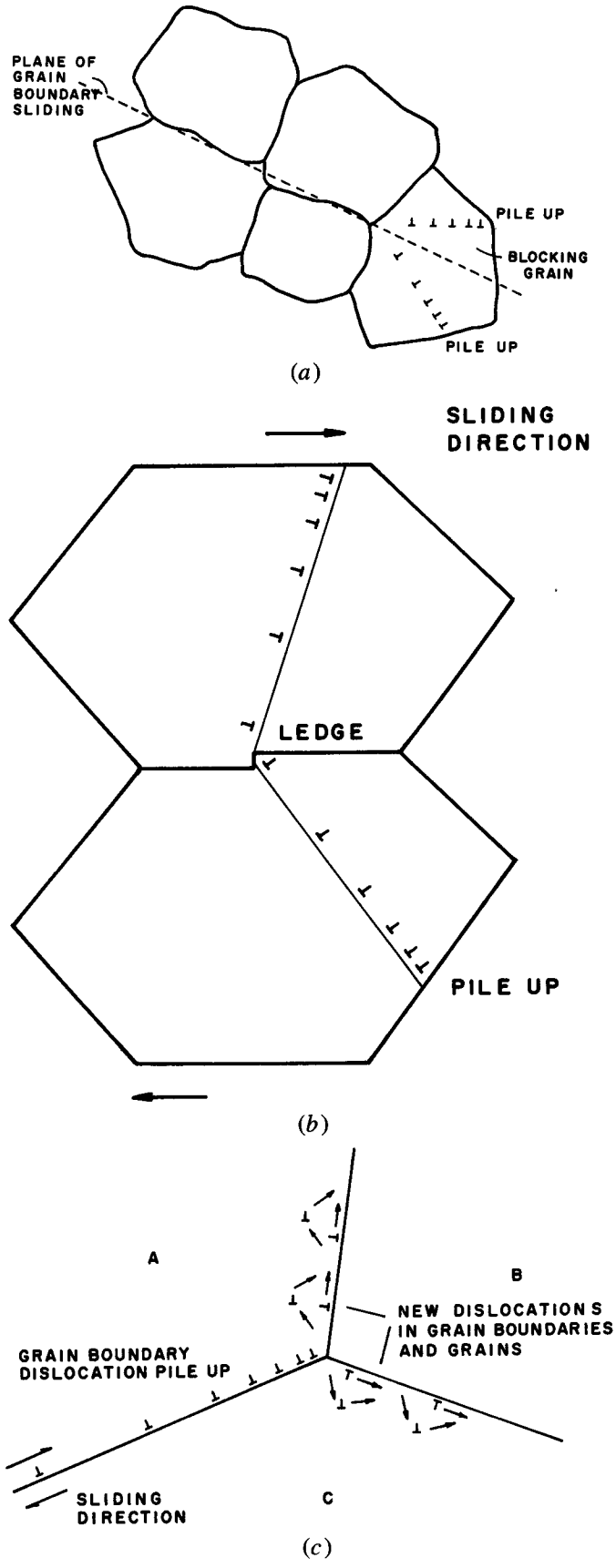

Fig. 4—Schematic illustrations (*a*) slip accommodation of grain boundary sliding,[26] (*b*) slip accommodation from grain boundary ledges,[27,28] and (*c*) core mantle theory[29] with accommodation by dislocation motion in and near the grain boundary.

produced by ledges and protrusions in the boundary (see Figure 4(b)). The pile-up concept was also used. Springarn and Nix[28] developed a similar model, but there were detailed differences in the mechanism of dislocation absorption and movement in the grain boundary.

Gifkins[29] treated GBS and accommodation in terms of the motion of grain boundary dislocations (see Figure 4(c)), an approach known as the core-mantle model. Accommodation at the triple junction was allowed by creating new dislocations at the stress concentration followed by their climb either in or near the grain boundaries. The core of the grain remained free of dislocations which were confined to the mantle, *i.e.*, the near grain boundary region. This theory was subsequently extended[30] to allow for the three-dimensional contribution of sliding of grains from in front and behind the switching event.

In a development of the core-mantle approach for a classical two-phase eutectic/eutectoid superplastic material, Gittus[31] treated the sliding process by motion of superdislocations in the interface. The unit process considered was the grain switching event discussed by Ashby and Verrall.[24] The pile-up was released by climb of the leading dislocation into the interphase grain boundary. It was essentially the same mechanism as illustrated in Figure 4(c), except that the lower grain *C* was the second phase.

All of these models predicted the following for region II:

1. A highly strain rate sensitive stress with maximum $m = 0.5$.
2. No large grain elongation; extensive GBS and grain rotation; significant dislocation motion, either throughout the grain or only in the mantle.
3. A significant dislocation density either within the grain or at grain and interphase boundaries.
4. Activation energies equivalent to grain boundary or interphase diffusion.

These theories accounted for all points in Section II except the high values of m, point 4, points 3, 7, and 10. Point 10 will be addressed later in section IV.

Only the theories of Gifkins and Gittus specifically addressed the question of operative mechanisms in region I. These were, respectively, GBS itself and pinning of dislocations to ledges in grain boundaries. It was implied in all cases, but not necessarily stated, that the mechanism in region III was conventional dislocation creep. In this region texture could be created, grains elongated, and GBS contributed less.

C. *Grain Boundary Sliding Rate Controlling (Figure 5)*

Beere[32,33] has treated the process of GBS itself as if it were controlling: the accommodation process was referred to as rapid diffusion creep. The core-mantle approach was taken, but the physical details of the sliding process were not considered. Deformation of an aggregate of cube grains was treated for different resistances to sliding at the boundaries. It was shown that, if one set of interfaces had a greater resistance to sliding, then a given strain could be achieved only by allowing the grains to rotate (see Figure 5). This explained the large number of observations[11] of reduction in texture produced by superplastic deformation.

Padmanabhan[34] has developed a similar theory of superplasticity in terms of a stress aided diffusion controlled, viscous grain boundary model. This was a development of a model for grain boundary shear due to Kê.[35] The process was treated as an atom vacancy exchange that lead to diffusion controlled flow in the boundary. The grains were treated as hard nondeformable cores with a viscous mantle (not necessarily Newtonian).

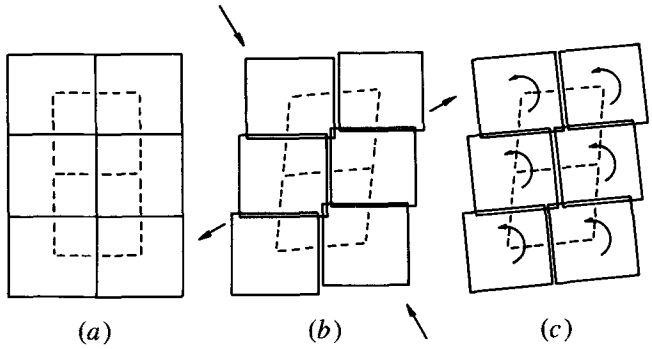

Fig. 5—Schematic illustrations of six square grains that are deformed[32] uniaxially producing (*b*) grain boundary sliding on all faces. Grain rotation (*c*) follows reduction of sliding on vertical boundaries for the same strain.

Both theories predict points 1, 2, 4, 5, 8, and 10 in section II, but the latter is open to serious criticism.[36,37]

D. *Conclusions*

None of the theories summarized here is entirely satisfactory. Many of the intrinsic defects in them have been discussed at length in the literature [11,12,30,33,36–40] and will not be repeated.

IV. REQUIREMENTS FOR SUCCESSFUL MICROSTRUCTURAL STUDIES

Optical metallography, scanning electron microscopy (SEM), transmission electron microscopy (TEM), and *in situ* high voltage electron microscopy (HVEM) have all been used to study the deformation mechanisms associated with superplasticity. In addition, cumulative changes in crystallographic texture with increased plastic strain have been studied to detect slip under the action of the applied stress. However, considerable care must be taken in conducting all of these experiments if the results are to provide useful information. Some of the factors that must be considered are discussed below.

1. To preserve any dislocation arrays or partially recrystallized regions for observation in TEM, the specimen should be quenched rapidly to room temperature, under load and without bending. Since loads are frequently <100 pounds and specimens are soft and thin, this presents a difficult experimental problem. Consequently, it has not been attempted very frequently. Note that dislocations typically need only move $\lesssim 1\ \mu$m to reach grain boundary sinks. Some success in combatting this problem has been obtained by generating a microstructure that contains fine precipitates which act as barriers to dislocation loss. This approach is discussed further in sections V-B, V-C, and VI-B.
2. If the observations[21,23] of sliding of groups of grains in Pb-Sn eutectic alloys are general, not all grain boundaries

slide simultaneously. Consequently, at any instant during deformation, there are only likely to be isolated regions of the specimen where dislocation accommodation is occurring. These may not be visible in a given thin foil. Furthermore, the history of any given electron transparent area is unknown. Thus, it is uncertain how long the region may have been "annealing out" dislocations at the deformation temperature after local GBS and accommodation stopped.

3. *"In situ"* deformation experiments in the HVEM must meet stringent conditions if the results are to be typical of bulk material.[41] Thus, the specimen must be at least four grains thick, the image must exhibit adequate contrast and intensity to resolve dislocations, and the deformation temperature must be high enough for thermally induced point defects to swamp those produced by the electron beam. These have not all been met in any of the *in situ* studies reported[42,43,44] to date.

4. Changes in texture provide useful information only if the complete texture is defined. If this is done, the technique can be valuable because the result is not susceptible to such factors as dislocation loss during loading and cooling. Furthermore, the texture measured after a given strain includes the cumulative effect of the complete deformation process, whereas classical metallographic techniques provide evidence only for the instantaneous contribution of a deformation process when the tensile test is stopped. Random grain rotation, recrystallization and slip should, in principle, be clearly identifiable. The former should result in continuous reduction in starting texture with increased plastic strain. Recrystallization should produce texture components that are readily identifiable from studies of recrystallization alone. *Slip in response to the applied stress* would be expected to stabilize individual grains in certain orientations as they reach them during random grain rotation. Such stabilization against further rotation may not be permanent for a given grain. Thus, different grains may contribute to a given texture component at different times during the tensile test. In contrast, accommodation slip in response to local stress concentration produced by GBS would not be expected to stabilize any texture component because the stresses would occur randomly over a range of directions.

Of course, independent results from different experimental approaches should be obtained to optimize the interpretation of the data from any given material.

V. MICROSTRUCTURAL STUDIES ON MODERN COMMERCIAL ALLOYS

Because classical superplastic alloys were based upon eutectic or eutectoid compositions, their mechanical properties were unsatisfactory for structural applications. Consequently, much research has been directed toward developing superplasticity in alloys with compositions close, or identical, to existing commercial materials. The physical principles have been summarized,[2] and their application has led to a new generation of alloys that were superplastic after the correct combination of hot and cold working in the two phase condition. Fine precipitates were used to pin grain boundaries and limit grain growth. However, it is only recently that the mechanisms of deformation in these materials have been studied. This section describes metallographic observations on the complex Ni-base alloy IN100, several Al-base alloys including Supral 150, and an Mg-base alloy, MA8. These materials have been selected not only because the results showed more complex phenomena than have been reported in the classical superplastic alloys, but also because several experimental techniques have been applied to the problem.

A. *Nickel-base Alloy IN100*

Powder metallurgy process routes provide excellent uniformity of composition and mechanical properties that have been difficult to achieve with conventional casting and forging techniques. Such powder consolidated alloys have been rendered superplastic by a process known as Gatorizing*

*Gatorizing is a registered trademark of the Pratt and Whitney Aircraft Corporation.

which involved extrusion below, but within 250 K of, the recrystallization temperature.[2] A large amount of deformation was introduced by the extrusion, and the adiabatic heating caused during the process raised the temperature high enough to allow dynamic recrystallization without excessive grain growth. During the whole process, the temperature was always substantially below the γ' solvus so the alloy was always two phase. The large volume fraction of γ' stabilized the fine grain size generated by dynamic recrystallization during the extrusion step.

The mechanical properties associated with superplastic IN100 have been well documented,[45-48] although the compositions, grain size, and exact details of the thermomechanical treatment were not identical in all studies. Nevertheless, all workers found maximum values of $m \simeq 0.5 \pm 0.5$, and high activation energies ($\sim 420 \pm 70$kJ/mol^{-1}) for region II. The latter were substantially greater than volume diffusion for various elements in nickel-base alloys (168 to 315 kJ/mol^{-1}).[49,50,51]

Metallographic studies have been few. It has been shown that γ' coarsens after superplastic deformation of IN100[45,46] and MAR-M-200.[52] It was also reported[47] that an increase in carbon and oxygen content led to increased precipitation of oxycarbides on prior particle boundaries, leading to improved local reduction in grain size. Kobayashi[53] demonstrated that superplastic deformation in IN100 was accompanied by a marked change in the γ' morphology. Initially, the microstructure consisted of γ' cubes in equiaxed γ grains. After small strains, precipitate denudation occurred along grain boundaries perpendicular to the tensile axis, while enhanced growth of γ' was observed on boundaries parallel to the axis. This was rationalized in terms of Nabarro-Herring creep. However, after larger strains, the precipitate free zones were randomly oriented relative to the tensile axis, presumably due to grain rotation. At strains of several hundred pct, the microstructure consisted of (~ 33 μm) equiaxed γ and γ' grains with little retention of the original $\gamma + \gamma'$ grains. These observations were consistent with a mechanism consisting of GBS with diffusion accommodation.

Very recently, extensive transmission electron microscopy studies have been made[54,55] of superplastically deformed powder consolidated and gatorized IN100 containing a medium level (0.076 wt pct) of carbon. The material was deformed in air at 1311 °C, then water quenched under zero

load. Regions I, II, and III were found in the $\ln \sigma$-$\ln \dot{\varepsilon}$ curve with maximum $m = 0.66$. Elongations of ~1000 pct were obtained, but were limited by the length of the hot zone in the furnace. The activation energy Q_σ at constant stress in region II was found to be 483 kJ/mol.[-1] Values of about half this were obtained at constant strain rate $Q_{\dot{\varepsilon}}$. A similar value was reported[56] for diffusion controlled dislocation motion in γ' in IN100 during creep.

The microstructure of the as-extruded material was complex. Three different types of area could be distinguished.

(a) Recrystallized γ/γ' grains containing very few dislocations (Figure 6(a)).
(b) Warm worked γ/γ' grains often containing a well recovered dislocation substructure (Figure 6(b)).
(c) Heavily worked regions of γ and γ' (Figure 6(c)).

The local variation of local dislocation densities was large and included regions that were fully recovered and others that were not; see Figure 6(d). In some cases acicular structures were also seen.

The heating sequence before beginning the tensile test did not significantly change the microstructure, except for a small amount of dislocation rearrangement. Although material annealed at 1311 °C for the time necessary to strain superplastically to 200 pct was partially recrystallized, a number of heavily worked regions remained (see *A* Figure 7(a)). In material deformed 200 pct the microstructure was still heterogeneous (see Figure 7(b)). Although the overall dislocation density was reduced compared to the starting material, heavily deformed areas *A* still remained. There was less secondary γ' visible and there was more agglomeration of γ' than was observed after annealing. Coherent twin boundaries, interphase γ/γ' boundaries and grain boundaries often contained a high density of dislocations; an example is shown in Figure 7(c). Grains where secondary γ' was present showed different effects. In some areas dislocations were present, providing evidence for dislocation motion during superplastic deformation. In others dislocations were not visible (Figures 7(a) and (b)).

Extensive microstructural studies of material deformed to several strains at different strain rates led to the conclusion that the deformation process in region II was complex. Several mechanisms appeared to be occurring simultaneously, including recrystallization, GBS and grain rotation, extensive diffusion, and dislocation motion. Dislocation motion played a smaller part at low strain rates in region I, but there was still evidence for its occurrence. Similarly, at the upper end of region II, near region III, dislocation motion was more important. In region III the evidence was consistent with dislocation creep. Clearly, in this material the single mechanisms outlined in Section III were not relevant and could not be related directly to the measured mechanical properties or activation energies.

B. *Al-base Alloys*

Most of these alloys have been made superplastic by small 0.5 wt pct Zr additions. Although other approaches exist, studies of the deformation mechanisms of these alloys have not been published. The zirconium precipitated as a finely dispersed intermetallic compound Al_3Zr, which pinned grain boundaries and limited grain growth. Work in

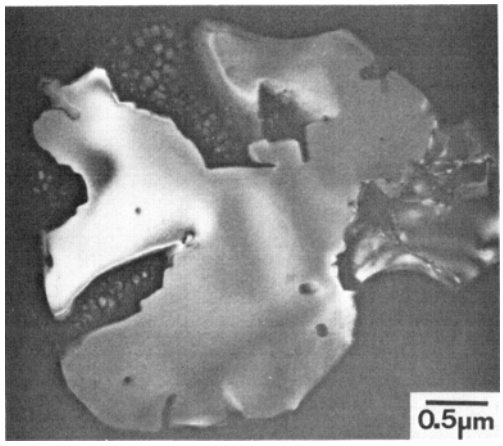

(*a*)

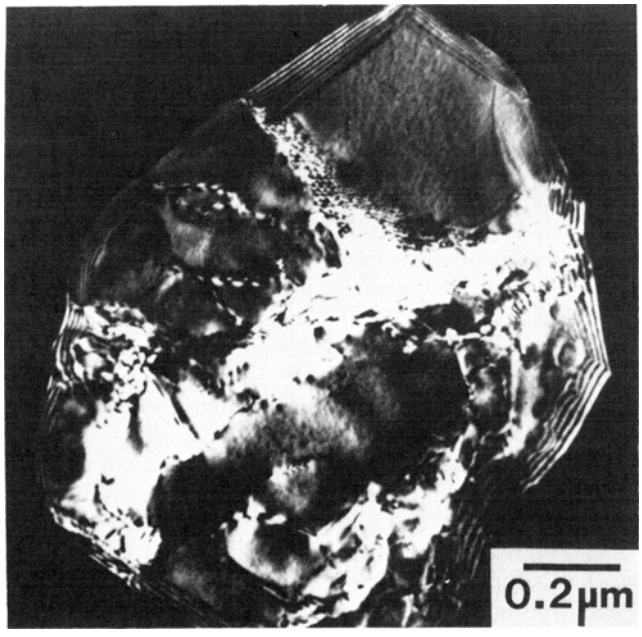

(*b*)

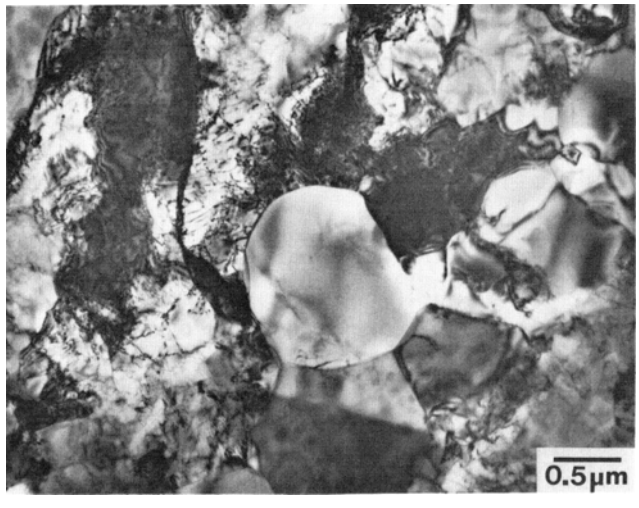

(*c*)

Fig. 6—Transmission electron micrographs from as "gatorized" IN100,[48] (*a*) dark field of recrystallized γ-γ' grain, superlattice reflection, (*b*) dark field recovered γ-γ' grain, matrix reflection, and (*c*) bright field warm worked region.

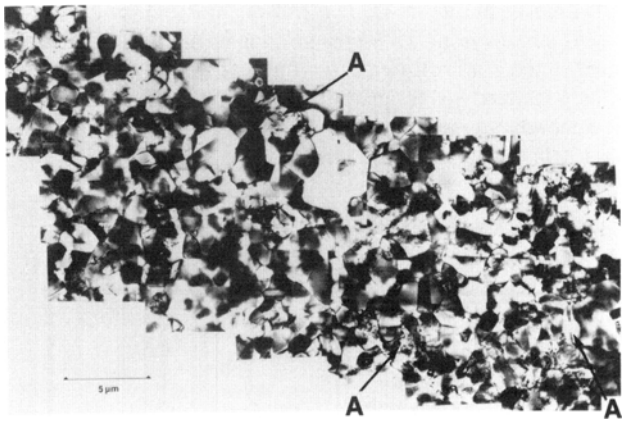

(*a*)

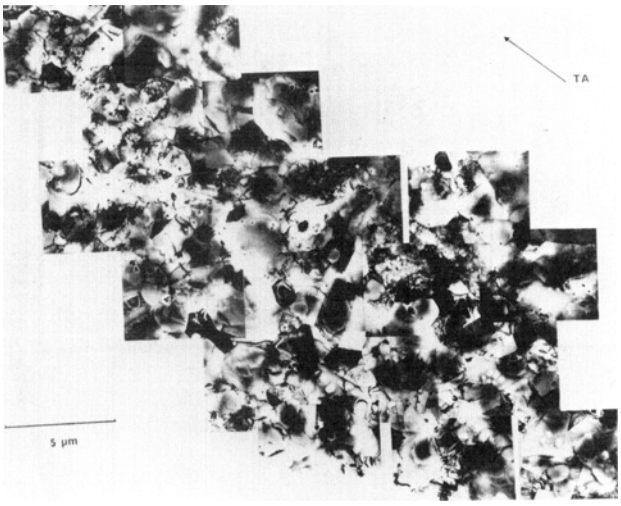

(*b*)

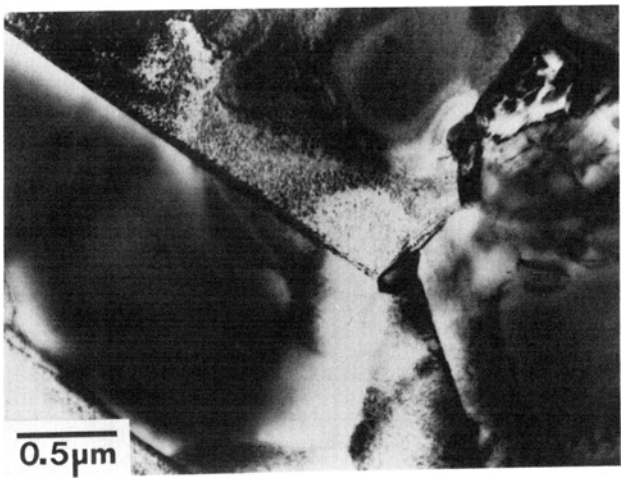

(*c*)

Fig. 7—Transmission electron micrographs for "gatorized" IN100[48] (*a*) annealed 4750 sec at 1038 °C; (*b*) 200 pct ε, $\dot{\varepsilon} = 4.3 \times 10^{-3}\text{sec}^{-1}$, $m = 0.66$; and (*c*) a coherent twin boundary with extrinsic dislocations. 200 pct ε, $\dot{\varepsilon} = 4.3 \times 10^{-3}\text{sec}^{-1}$ $m = 0.66$ with extrinsic dislocations. *A* denotes heavily warm worked region.

developing these alloys has been concentrated primarily in two groups. Matsuki and his co-workers[57–62] have studied the effect of small (0.3 to 0.4 wt pct) Zr additions to Al-Zn-Mg, Al-Cu, and Al-Mg alloys. In these cases the fine grain size was produced by recrystallization after thermomechanical processing and prior to testing. A slightly different approach has been taken by Stowell, Grimes, and their co-workers[63–68] in Al-Cu-Zr, Al-Zn-Zr, and Al-Mg-Zr alloys. Here the micrograin requirement was produced by thermomechanical processing, but the material was tested immediately so that there was dynamic recrystallization during the early stages of superplastic deformation. Extensive metallographic studies have been conducted on all of these alloys with the aim of identifying operative mechanisms.

1. *Al-6 wt pct Mg ~1 wt pct ZrMnCr (Recrystallized)*

The microstructure was fully recrystallized,[59] and both fine Al_3Zr particles and coarse $Al_{18}Cr_2Mg_3$ or $(MnCr)Al_7$ particles were present. The stress-strain rate relationship was sigmoidal with maximum m ~0.6 and superplasticity was found in the temperature range 430 to 520 °C. Elongations ranged from 245 pct at 400 °C to 885 pct at 530 °C. GBS was detected as a major deformation mode in region II, using optical metallography. This was confirmed by the overall reduction in crystallographic texture imposed by superplastic deformation. TEM of superplastically deformed material demonstrated that a high density of dislocations was present in some of the grains, without cell formation, under straining conditions corresponding to maximum m. Slip at maximum m was confirmed by observation of changes in the (013) [100] components of the texture with increasing superplastic strain as a function of test specimen orientation relative to the rolling direction. These results were consistent with a deformation mechanism consisting of GBS accommodated by dislocation motion within the grains.

2. *Al-9 wt pct Zn-1 wt pct Mg-0.22 wt pct Zr (Recrystallized)*

In a similar approach to that outlined above, Matsuki, *et al*[60] showed direct evidence for grain switching events involving grain boundary sliding and grain rotation. Texture measurements were reported for deformation at maximum m and interpreted in terms of dislocation motion. It was again concluded that the deformation process was GBS with accommodation by dislocation motion.

3. *Al-x wt pct Cu-0.22 wt pct Zr (Recrystallized)*

In a study[62] of several Al-Cu alloys containing different amounts of $CuAl_2$, it was concluded that the superplastic deformation could be explained in terms of GBS with accommodation by slip in the Al (α) phase and diffusion in the θ $CuAl_2$ phase. Dislocations were observed in many grains by TEM after deformation at maximum m. This was true for both the 6 wt pct Cu-0.22 wt pct Zr and the 33 wt pct Cu-0.18 pct Cr-0.16 pct Mn alloy, which both contained fine intermetallic precipitates. The stability of the ⟨100⟩ aluminum texture component with increased strain at maximum m confirmed the importance of dislocation motion in superplastic deformation of this material.

4. *Al-6 wt pct Cu-0.5 wt pct Zr, Supral 150 (Worked)*

In the more complex case of the Zr containing alloys that recrystallize during deformation, TEM evidence was obtained

for dislocation motion during superplastic deformation at maximum m. In addition, detailed studies[69] have been made of changes in individual components in the texture accompanying superplastic deformation in an alloy similar to Supral 150.* Crystallite orientation distribution functions (CODF) were used to characterize the texture.

*Supral 150 is the registered name for an Al-6 wt pct Cu-0.5 wt pct Zr alloy manufactured by T. I. Superform Metals.

The C. O. D. F.[70,71] expresses the probability of a crystallite having an orientation with respect to the specimen axes in terms of the three Euler angles ψ, θ, and ϕ. The specimen axes normally chosen are the rolling, normal, and transverse directions of the sheet, and ψ, θ, and ϕ are defined as in Figure 8. Probabilities are then expressed as x random in Eulerian space, conventionally displayed at constant ϕ sections. In the case of cubic materials, a complete texture description can be made in a region of Eulerian space defined by $0 < \psi, \theta$, and $\phi < \pi/2$. Charts for the analysis of such C. O. D. F. plots in terms of ideal orientations have been published by Davies *et al.*[72] A full description of the C. O. D. F. representation of texture may be found in the above references. For the present purposes, however, it is necessary only to note that the texture data is displayed on a rectangular chart of constant ϕ with ψ and θ varying along the x and y axes from 0 to $\pi/2$. A particular point on any section corresponds to a specific component of the texture. Figure 9 shows the important ideal orientations in the $\phi = 0$ section of the C. O. D. F. for a cubic crystal structure.

It was found to be possible [69] to separate the effects of GBS, single and multiple slip, and dynamic recrystallization on the texture changes. Some of the results are summarized in Sections (a) and (b) below.

(a) *Texture Measurements Showing Recrystallization*

Figure 10 shows the complete C. O. D. F. for the as-received material before superplastic deformation. The initial texture was chiefly composed of a tube of preferred orientation running from $(101)\langle\bar{2}32\rangle$ in the $\phi = 0$ deg section, to near $(113)\langle\bar{3}32\rangle$ in the $\phi = 45$ deg, and from $(\bar{1}10)\langle\bar{2}23\rangle$ in the $\phi = 45$ deg section to $(011)\langle\bar{3}22\rangle$ in the $\phi = 90$ deg section. This was similar in nature to the tube formed in the cold rolling of fcc metals, which Kallend and Davies[73] showed to be attributable to multiple $\{\underline{1}11\}\langle 1\bar{1}0\rangle$ slip. Secondary components were also visible at $(\bar{1}01)\langle 010\rangle$, $(\bar{1}03)\langle 301\rangle$, and $(30\bar{1})\langle 103\rangle$ in the $\phi = 0$ section.

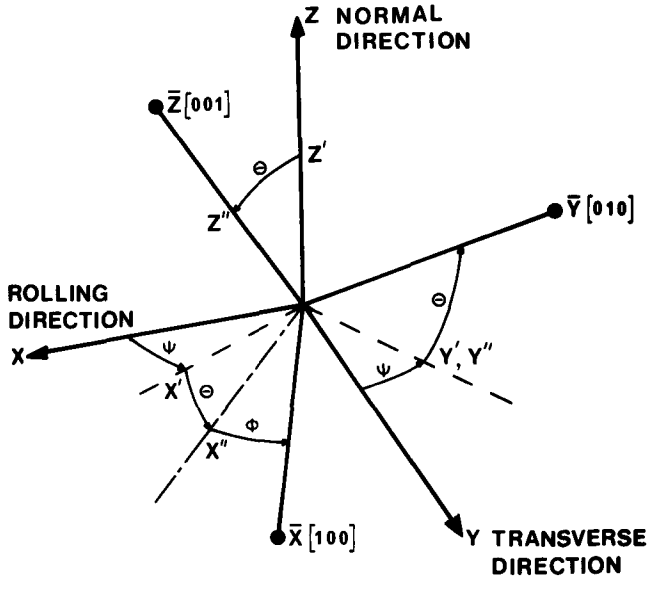

Fig. 8—A diagram relating the crystallite axes $\bar{x}$, $\bar{y}$, and $\bar{z}$ to the imposed specimen axes x, y, and z through the three Euler angles ψ, θ, and ϕ.

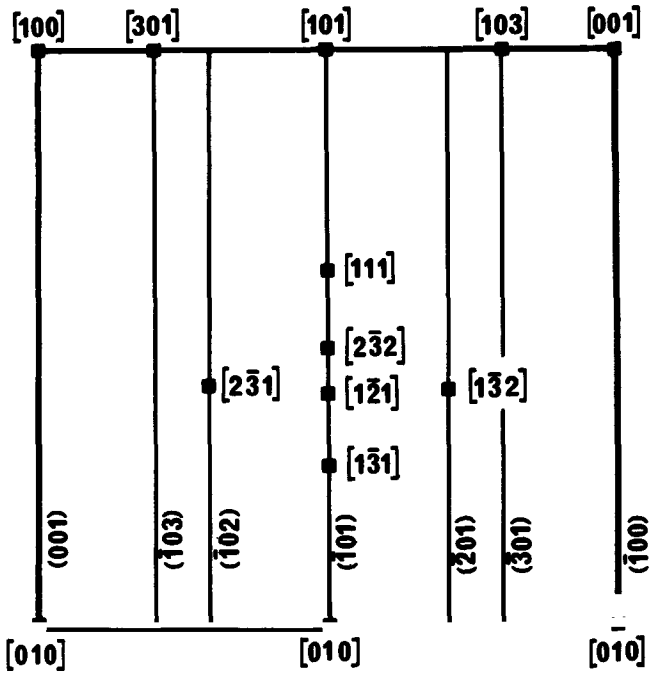

Fig. 9—The important planes and ideal orientations occurring in the $\phi = 0$ section of the C. O. D. F.

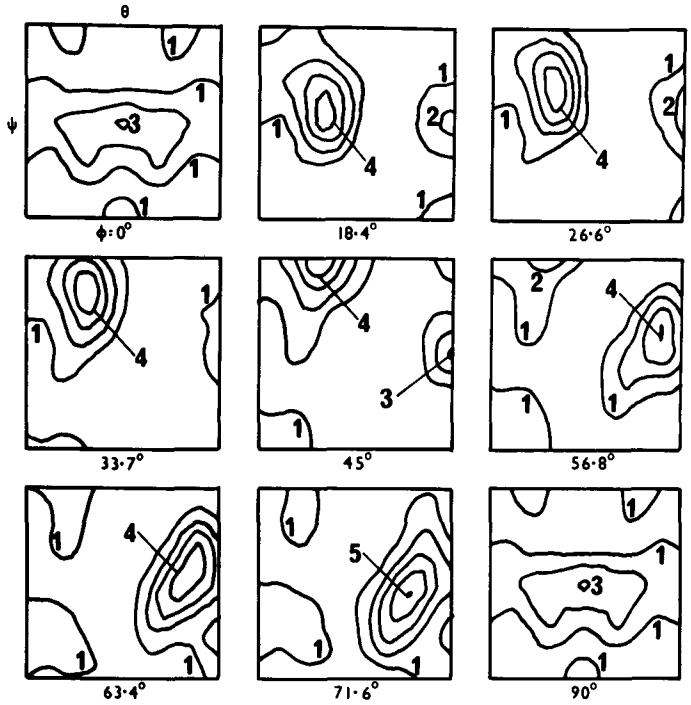

Fig. 10—The C.O.D.F.[69] of the as-rolled Al-6 pct Cu-0.5 pct Zr presented in sections of constant ϕ indicated.

Although all sections of the C. O. D. F. were required for the complete analysis, the $\phi = 0$ sections can be used to illustrate the occurrence of recrystallization during annealing and superplastic deformation. Consider first the effect of annealing alone (see Figure 11).

Figure 11(a) *Material heated to 450 °C, the tensile test temperature*. There was little change in texture. Only very slight sharpening was noted throughout the tube, except in the $\phi = 0$ section where there was a decrease around $(\bar{1}01)\langle 2\bar{3}2\rangle$, and the peak formerly present there was lost while two new peaks were noted developing at $(\bar{1}02)\langle 2\bar{3}1\rangle$ and $(\bar{2}01)\langle 1\bar{3}2\rangle$. A decrease in intensity in the $\phi = 0$ section was also noted for orientations running from $(\bar{1}01)\langle 1\bar{2}1\rangle$ to $(\bar{1}01)\langle 1\bar{3}1\rangle$.

Figure 11(b) *Material annealed for one hour*. Annealing for this period led to a further slight increase in texture sharpness. The components at $(\bar{1}03)\langle 301\rangle$, $(\bar{3}01)\langle 103\rangle$ were strengthened, the decline in material around $(\bar{1}01)\langle 1\bar{3}1\rangle$ was halted, and the build-up of the new peaks at $(\bar{1}02)\langle 2\bar{3}1\rangle$ and $(\bar{2}01)\langle 1\bar{3}2\rangle$ continued.

Figure 11(c) *Material annealed for seven hours*. Annealing for the period of the longest tensile test produced a fall in the overall level of texture, although the tube orientations were preserved, but weakened in parts. Cube orientations were now apparent, while the separate peaks at $(1\bar{0}3)\langle 301\rangle$ and $(\bar{3}01)\langle 103\rangle$ were lost. The splitting of the tube observed on annealing for shorter times was not seen, and instead a well-developed peak at $(\bar{1}01)\langle 2\bar{3}2\rangle$ was observed, as in the starting material.

The results described above show that two distinct types of behavior occurred. Firstly, on short anneals, there was peak splitting with a consumption of material in orientations from $(\bar{1}01)\langle 1\bar{3}1\rangle$ to $(\bar{1}01)\langle 2\bar{3}2\rangle$, and an increase at $(\bar{1}02)\langle 2\bar{3}1\rangle$ and $(\bar{2}01)\langle 1\bar{3}2\rangle$, which was coupled with a general increase in the tube. Secondly, after an anneal of seven hours at 450 °C, intensity was once again increased at the $\phi = 0$ end of the tube, and the peak splitting was no longer noted. An emergence of the characteristic cube texture, often noted on the discontinuous recrystallization of cold rolled fcc metals[74] was seen here.

An examination of the C. O. D. F.'s of material deformed superplastically to a strain of 25 pct revealed both sharpening of the texture and splitting of the orientation tube in the $\phi = 0$ section. These effects were in line with the changes seen on short static anneals (up to one hour at 450 °C). Hence, it was concluded that dynamic recrystallization occurred during superplastic deformation of this alloy. There was no evidence of the changes produced on long static anneals, *e.g.*, the formation of a cube component; thus, the dynamic recrystallization was of the type produced by short static annealing.

A comparison of the specimens deformed to 250 pct elongation, either parallel or transverse to the rolling direction, allowed a further insight into the nature of the dynamic recrystallization process. It was found that the splitting of the tube noted in specimens pulled parallel to the rolling direction was (a) completely suppressed on straining in a transverse direction, with $\dot{\varepsilon} = 10^{-2}\ s^{-1}$, (b) almost suppressed at $\dot{\varepsilon} = 10^{-3} s^{-1}$, and (c) again noticeable at $\dot{\varepsilon} = 10^{-4}\ s^{-1}$ (see Figure 12). Clearly, the direction of applied stress influenced the manner in which recrystallization occurred. Although the motion of the high angle grain boundaries is not expected to be stress coupled, that of subboundaries is.[75,76] Hence, it was concluded that the formation of the recrystallization texture involving the splitting of the skeleton tube took place by stress assisted movement of subboundaries. Watts, *et al*[67] have drawn a similar conclusion based upon TEM studies of a similar Al-Cu-Zr alloy.

(b) *Texture Measurements Showing Slip*

Evidence was provided, by the observed stabilization of $(101)\langle 11\bar{2}\rangle$ orientations, that single slip occurred in some of the grains in specimens deformed in region II at maximum *m in response to, and in directions governed by, the applied tensile stress*. Such slip was independent of any occurring as a local accommodation mechanism for grain boundary sliding and strongly implied that accommodation of grain boundary sliding occurred by dislocation motion. There was no evidence for slip in region I.

It should also be noted that this material exhibited severe mechanical anisotropy.[77] Detailed study of the texture changes produced by deformation in region III confirmed the above identification of slip mechanisms in region II.

(c) *TEM Studies Showing Recrystallization and Slip*

TEM studies[67,78] have provided direct evidence for continuous recrystallization of the type defined above. TEM evidence[77] for dislocation activity in region II at maximum m is shown in Figure 13.

5. *Conclusions*

It was clear that dislocation activity played a significant role in regions II and III. This occurred in region II, not only in direct response to the applied stress, but also by inference as an accommodation mechanism for local stress concentrations produced by GBS. It was also clear that superplastic deformation could occur when dynamic recrystallization was superimposed upon GBS and dislocation motion. Indeed, dynamic recrystallization may have acted as a further accommodation process by removing regions of high dislocation density. For these complex alloys, a full description of superplasticity could not be found in any one of the theories outlined in Section III, although those mechanisms

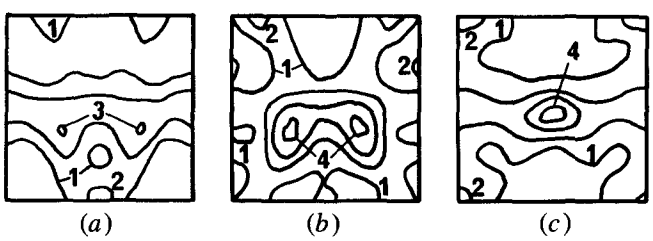

(a) (b) (c)

Fig. 11—the $\phi = 0$ sections of the C. O. D. F.'s[69] of the Al-6 pct Cu-0.5 pct Zr alloy following various anneals (*a*) taken to 450 °C and equilibrated, (*b*) 1 h at 450 °C, (*c*) 7 h at 450 °C.

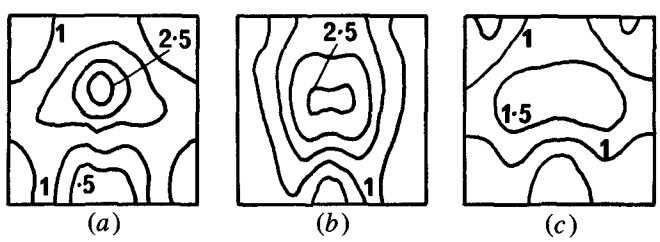

(a) (b) (c)

Fig. 12—The $\phi = 0$ sections of the C. O. D. F.'s[69] of the Al-6 pct Cu-0.5 pct Zr alloy deformed transversely to the rolling direction to 250 pct strain (*a*) $\dot{\varepsilon} = 10^{-3}\text{sec}^{-1}$ $m = 0.5$ and (*c*) $\dot{\varepsilon} = 10^{-4}\text{sec}^{-1}$ $m = 0.3$.

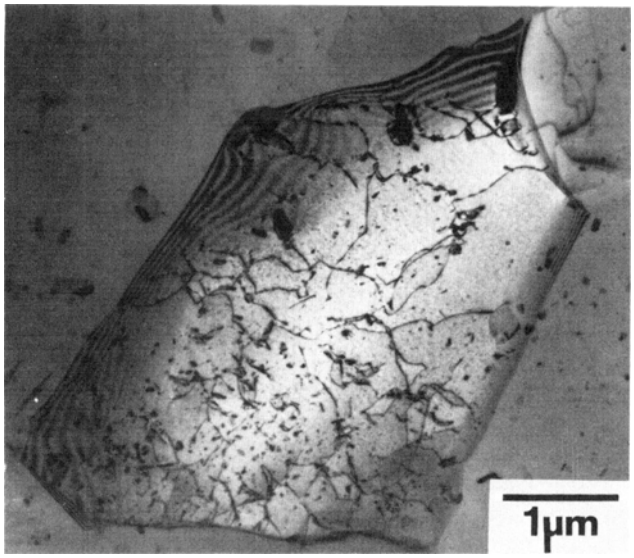

Fig. 13—Dislocations in a grain in Al-6 pct Cu-0.5 pct Zr[78] in material deformed to 75 pct elongation $\dot{\epsilon} = 10^{-3}\text{sec}^{-1}$ region II.

including dislocation motion in the bulk of the grain undoubtedly played a part.

C. *Magnesium-Base Alloy MA8*

In a series of papers[79,80,81] on the commercial magnesium alloy MA8 (Mg-1.5 pct Mn-0.3 pct Ce) both GBS and significant dislocation motion were reported throughout region II. The evidence was based on texture studies with complete pole figures and TEM studies of superplastically deformed material. Direct observation was facilitated by the presence of fine precipitates that appeared to pin dislocations within the grains and prevent loss to grain boundaries. It was suggested that lattice dislocations interacted with grain boundaries leading to an enhancement of the boundary diffusion coefficient.

VI. MICROSTRUCTURAL STUDIES ON THE Zn-Al EUTECTOID ALLOY

This is a well-known superplastic material with the fine grain size stabilized by approximately equal volume fractions of each phase present. Its mechanical properties have been reviewed by Langdon[17] in a companion paper. The material forms the basis for commercial superplastic alloys[2] and has also been one of the most extensively studied of the classical eutectoid or eutectic alloys. The results were sometimes conflicting, although this can be resolved, as shown in Sections VI-A through VI-C.

Surface studies[26] have shown that there was no evidence of slip lines in material deformed in region II. However, there were sharp scratch offsets at grain boundaries,[82] although Ball and Hutchison[26] reported that these may be curved, indicating significant grain deformation. New surface was created at grain boundaries, indicating that grains are moving in and out of the surface. The contribution of GBS to the total strain was high, ~60 pct.[82]

Optical and electron microscopy studies have shown[82,83,84] that the fine grain size was stable throughout the tensile test in region II. Deformation in regions I and II led to limited grain growth (approximately times two at 500 pct strain), whereas direct annealing at the deformation temperature did not.[83,85-88] There was evidence for clustering of the grains of the same phase at large strains.[83,85] Grain and interphase boundaries tended to become curved, whereas they were straight before deformation.

A. *TEM and HVEM Studies Not Providing Evidence for Slip*

In one study[84,89] an attempt was made to use metastable α' particles in the α phase of this alloy to prevent dislocation loss to grain boundaries during unloading and cooling the tensile specimen. However, dislocations were not observed and it was concluded that slip was unimportant. Unfortunately, it was not clear whether, in fact, the α' particles were effective barriers to dislocations,[90,91] so the interpretation of the data was in question. Nevertheless, two useful results were produced by this study. Firstly, the precipitate size and distribution in the centers of the grains were unaltered by superplastic deformation, a clear indication that dynamic recrystallization had not occurred. Secondly, precipitate free zones developed near the grain boundaries, which implied that the accommodation process was confined to near grain boundary regions.

An *in situ* HVEM study[42] also failed to provide evidence for dislocation motion. However, grain switching events of the type and described in Section III-A were observed (see Figure 15). Unfortunately, this experiment did not meet the stringent conditions (outlined in Section IV) required for the results to be typical of the bulk material.[41] Damage from the electron beam probably enhanced diffusion locally[69] so that diffusion accommodation of GBS would be perferred over dislocation motion. Furthermore, the results were not typical of the bulk material because the specimen was only two to three grains thick.[93] Finally, the resolution of the pictures was probably inadequate to observe dislocations in the thickest regions.[41] This result was therefore not typical of bulk superplastic deformation.

B. *TEM Studies Providing Evidence for Slip*

The precipitate marker experiment was repeated[94,95] using zinc precipitates, and dislocation activity was found after superplastic deformation in material quenched under load. Figure 14 shows dislocations present after deformation in region II. At the lowest strain rates, below maximum m, the number of independent Burgers vectors was insufficient to satisfy grain compatibility requirements; it was concluded that diffusional processes became important. However, at and above maximum m enough Burgers vectors were available to satisfy grain compatibility. The results were consistent with a deformation mechanism involving accommodation of grain boundary sliding by dislocation motion.

C. *Texture Studies Providing Evidence for Slip*

Studies of partial[96] and complete[97-100] single pole figures were consistent with the occurrence of slip in region II in the zinc-rich phase. A detailed investigation[101] of the influence on the complete crystallographic texture of superplastically deformed material provided direct evidence for the occurrence of slip in both the zinc-rich, and the aluminum-rich,

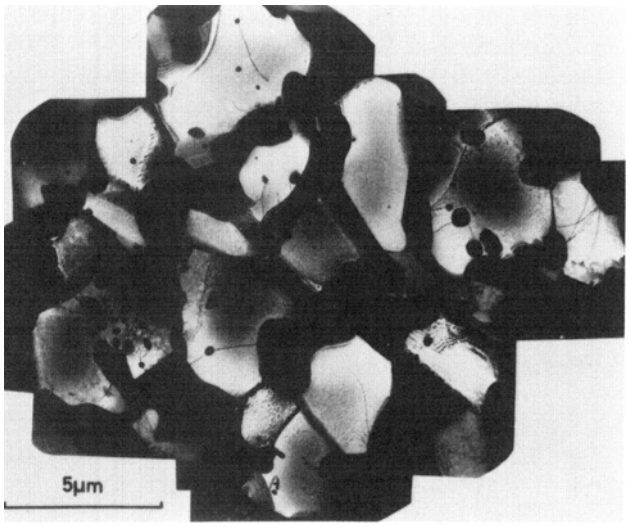

Fig. 14—A transmission electron micrograph[95] of Zn-40 wt pct Al deformed 190 pct strain, $\dot{\varepsilon} = 3 \times 10^{-4}\text{sec}^{-1}$, $m = 0.46$. Note dislocations pinned by precipitates, and in grain boundary.

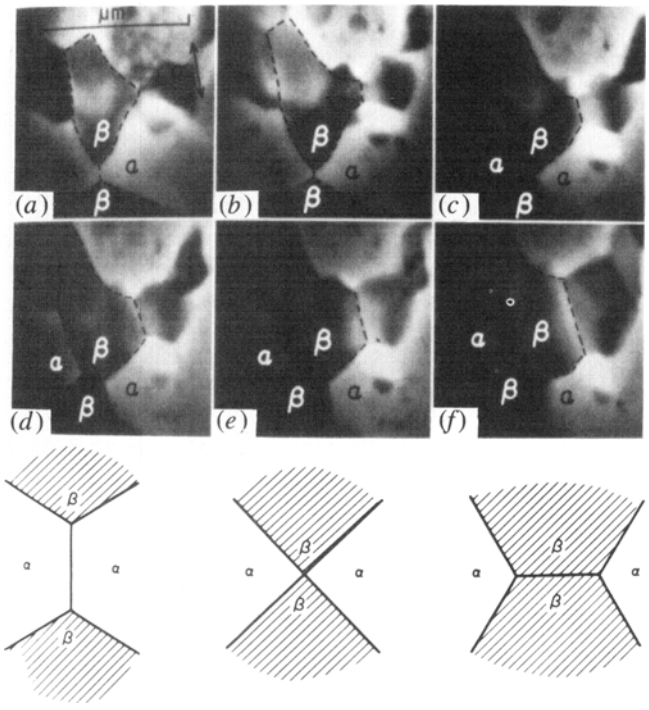

Fig. 15—Still micrographs[92] at increasing time intervals during the tensile straining of a thin Zn-Al eutectoid foil in the HVEM. 1 MeV, 18.5 NM/m^2, 100 °C (*a*) 38 min; (*b*) 44 min; (*c*) 49 min; (*d*) 53.5 min; (*e*) 56.5 min; (*f*) 63.5 min. The grain boundary configuration changes are shown schematically below the micrographs.

phases. C. O. D. F.'s were used to specify the texture. The alloy was near, but not at, the eutectoid composition.

Figure 16 shows the results that were interpreted in terms of slip in the aluminum-rich phase. It contains $\phi = 0$ sections of the C. O. D. F. for material deformed 100 pct at different strain-rates, together with the starting material and that annealed for one hour at the deformation temperature. After deformation at all strain-rates, the overall level of texture was reduced, which was shown by a general reduction in orientation density of the C. O. D. F.—compare Figure 16(a) with (b) to (d). The rate of removal of texture increased with decreased strain-rate, *i.e.*, toward maximum m.

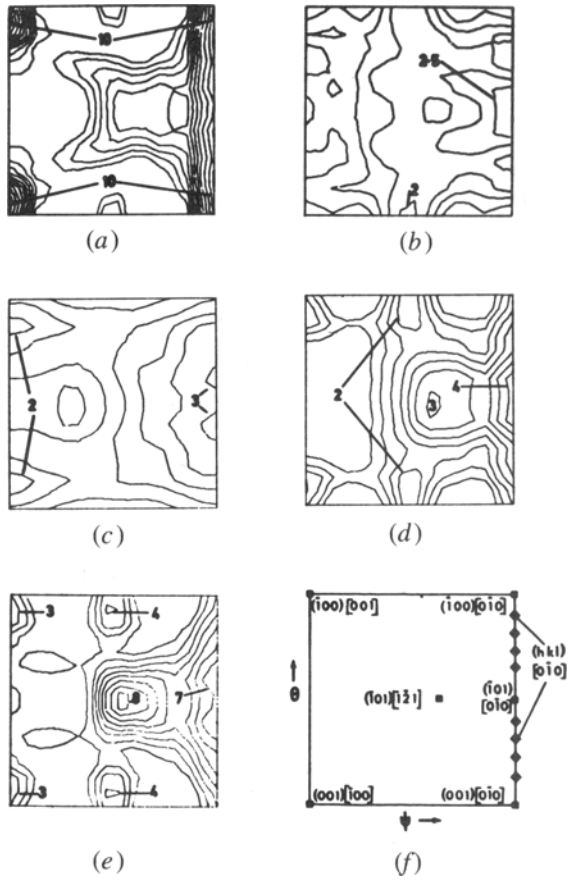

Fig. 16—The measured $\phi = 0$ sections of the crystallite orientation distribution function[101] for the aluminum-rich phase (units times random). (*a*) starting material; (*b*) deformed 100 pct $\dot{\varepsilon} = 3 \times 10^{-2}\text{min}^{-1}$; (*c*) deformed 100 pct $\dot{\varepsilon} = 3 \times 10^{-1}\text{min}^{-1}$; (*d*) deformed 100 pct $\dot{\varepsilon} = 3\ \text{min}^{-1}$; (*e*) annealed 1 h 270 °C; (*f*) a schematic diagram showing the position of certain ideal orientations in the $\phi = 0$ section.

Figure 16(f) shows the positions of the important components of texture in the $\phi = 0$ section. By comparing the peak positions in the measured sections in Figures (a) to (e), it was concluded that:

1. Only after deformation at the highest strain-rate was the peak in orientation density near $(\bar{1}01)\langle 1\bar{2}1\rangle$ retained.
2. The $(\bar{1}01)\langle 0\bar{1}0\rangle$ orientation was prominent in all deformed specimens, but less marked than in the starting material.
3. The initial strong cube component $\{100\}\langle 001\rangle$ of the texture was rapidly removed at all strain-rates.
4. By comparison of Figures 16(a) and (e) it can be seen that annealing strengthened the $(\bar{1}01)\langle 1\bar{2}1\rangle$ orientation, but weakened the cube texture.

The retention of specific components may be attributed to stabilization by slip of grains in these orientations for a limited period during the test. Thus, $(\bar{1}01)\langle 0\bar{1}0\rangle$ was stable during slip deformation (Figure 16(d)), and this region of Figures 6(b) and (c) showed that slip was important at all strain-rates investigated, including maximum m. Nevertheless, its contribution decreased with decreased strain-rates.

However, $(\bar{1}01)[1\bar{2}1]$ was retained only at high strain-rates, and this was part of a range of orientations stable during multiple slip in fcc materials deformed in plane strain.[102] The retention of this component at the highest strain-rate only, indicated that overall multiple slip occurred only in region III. At lower rates, slip occurred in isolated grains, which thus deformed rather like single crystals. Less than five independent slip systems were needed because diffusion accommodated grain boundary sliding could assist in maintaining grain compatibility.[95] The C. O. D. F. has also been used to study the Al-rich phase of the Zn-Al eutectoid alloy. It was found[103] that, after superplastic deformation to 200 pct strain, the texture had changed and slip-stabilized orientations were present.

Based upon all the work reported above, it was clear that extensive GBS occurred in region II with a lesser amount in region III. Profuse slip occurred in region III with decreasing amounts of slip as the strain rate is reduced in region II. Nevertheless, significant slip occurred *in response to the applied load* at maximum m. Consequently, slip should also be active as an accommodation process for stress concentrations produced by grain boundary sliding.

D. *Conclusions*

Bearing in mind the difficulties in conducting TEM and HVEM studies of superplasticity outlined in Section IV, it is considered that those experiments that did not observe dislocation motion did not constitute strong evidence for its absence. Indeed, the bulk of the evidence strongly indicated that dislocation motion occurred at maximum m in isolated grains *under the action of the applied stress* (texture and TEM studies). Furthermore, this implied some dislocation motion to accommodate stress concentrations arising from GBS. At very low $\dot{\varepsilon}$ both dislocation motion and diffusion contributed to accommodation of GBS (TEM, texture studies). However, it was not possible to differentiate among the theories described by Ball and Hutchison,[26] Mukherjee,[27] and Gifkins.[28]

VII. CONCLUSIONS

Microstructural studies of several commercially available alloys have led to the following conclusions for superplastic deformation at maximum m.

1. Depending upon the material, different combinations of processes may contribute to deformation.
2. GBS is important in all alloys reviewed here, *i.e.*, IN100, Supral 150, and similar Al-base alloys, MA8, the Zn-Al eutectoid, and related compositions.
3. Dynamic recrystallization occurs in IN100 and Supral 150.
4. Dislocation motion occurs, both directly under the action of the applied stress and as an accommodation process for GBS, in IN100, Supral 150, and similar Al-base alloys, MA8, the Zn-Al eutectoid, and related compositions.
5. Diffusion occurs in IN100, Supral 150, and Zn-Al alloys of eutectoid and near eutectoid compositions.
6. The contribution of individual deformation processes to the total strain has not been measured except for a few examples of GBS.
7. The rate controlling process is not in general identified by microstructural studies.
8. Because of the nature of superplastic deformation, considerable care must be taken in conducting TEM and HVEM studies if the results are to be relevant to deformation of bulk material.

ACKNOWLEDGMENTS

It is a pleasure to acknowledge the financial support of both the Science Research Council (UK) and the University of Delaware.

REFERENCES

1. M. M. I Ahmed and T. G. Langdon: *Metall. Trans. A*, 1977, vol. 8A, p. 1832.
2. J. W. Edington: *Met. Tech.*, 1976, vol. 2, p. 138.
3. C. E. Pearson: *J. Inst. Met.*, 1934, vol. 54, p. 111.
4. E. E. Underwood: *J. Metals*, December 1962, vol. 14, p. 914.
5. W. A. Backofen, I. R. Turner, and D. H. Avery: *Trans. ASM*, 1964, vol. 57, p. 980.
6. D. H. Avery and W. A. Backofen: *Trans. ASM*, 1965, vol. 57, p. 980.
7. D. H. Avery and W. A. Backofen: *ibid*, 1966, vol. 59, p. 359.
8. D. A. Holt and W. A. Backofen: *Trans. ASM*, 1966, vol. 59, p. 755.
9. W. A. Backofen, G. S. Murty, and S. W. Zehr: *Trans. TMS-AIME*, 1968, vol. 242, p. 329.
10. S. W. Zehr and W. A. Backofen: *Trans. ASM*, 1968, vol. 61, p. 30
11. J. W. Edington, K. N. Melton, and C. P. Cutler: *Prog. Mat. Sci.*, 1976, vol. 21, p. 61.
12. A. K. Mukherjee: *Ann. Rev. Mat. Sci.*, 1979, vol. 9, p. 191.
13. D. M. R. Taplin, G. L. Dunlop, and T. G. Langdon: *Ann. Rev. Mat. Sci.*, 1979, vol. 9, p. 151.
14. A. Ghosh and H. Hamilton: *Metall. Trans. A*, 1982, vol. 13A, p. 733.
15. E. W. Hart: *Acta Met.*, 1967, vol. 15, p. 351.
16. T. Hirano, M. Iharagi, M. Yamaguchi, and T. Yamane: *Metall. Trans. A*, 1975, vol. 6A, p. 2159.
17. T. G. Langdon: *Metall. Trans. A*, 1982, vol. 13A, p. 689.
18. T. G. Langdon: *J. Microsc.*, 1979, vol. 116, pt. 1, p. 47.
19. D. Lee: *Acta Met.*, 1969, vol. 17, p. 1057.
20. T. H. Alden: *Acta Met.*, 1967, vol. 15, p. 469.
21. D. J. Dingley: *Proc. 3rd Ann. SEM Symp.*, Pub. I. I. T., Research Inst., Chicago, IL 60616, 1970, p. 329.
22. A. E. Geckinli and C. R. Barrett: *J. Mat. Sci.*, 1976, vol. 11, p. 510.
23. N. Furushiro and S. Hori: *Scripta Met.*, 1979, vol. 13, p. 653.
24. M. F. Ashby and R. A. Verrall: *Acta Met.*, 1973, vol. 21, p. 149.
25. R. Z. Valiev and O. A. Kaibyshev: *Phys. Stat. Sol.*, 1978, vol. 45A, p. 77.
26. A. Ball and M. M. Hutchison: *Met. Sci. J.*, 1969, vol. 3, p. 1.
27. A. K. Mukherjee: *Mat. Sci. Eng.*, 1971, vol. 8, p. 83.
28. J. R. Springarn and W. D. Nix: *Acta Met.*, 1979, vol. 27, p. 171.
29. R. C. Gifkins: *Metall. Trans. A*, 1976, vol. 7A, p. 1225
30. R. C. Gifkins: *J. Mat. Sci.*, 1978, vol. 13, p. 1926.
31. J. H. Gittus: *Trans. ASME, J. Eng. Mat. and Tech.*, 1977, vol. 99, p. 244.
32. W. Beere: *J. Mat. Sci.*, 1977, vol. 12, p. 2093.
33. W. Beere: *Philos. Trans. R. Soc.*, London, 1978, vol. A228, p. 177.
34. K. A. Padmanabhan: *Mat. Sci. Eng.*, 1977, vol. 29, p. 1.
35. T. S. Kê: *J. Appl. Phys.*, 1949, vol. 20, p. 274.
36. R. C. Gifkins and T. G. Langdon: *Mat. Sci. Eng.*, 1978, vol. 36, p. 27.
37. R. C. Gifkins and T. G. Langdon: *Mat. Sci. Eng.*, 1979, vol. 40, p. 293.
38. A. Arieli and A. K. Mukherjee: *Metall. Trans. A*, 1982, vol. 13A, p. 717.
39. J. R. Springarn and W. D. Nix: *Acta Met.*, 1978, vol. 26, p. 1389.
40. M. F. Ashby, G. H. Edward, J. Davenport, and R. A. Verrall: *Acta Met.*, 1978, vol. 26, p. 1379.
41. R. H. Bricknell and J. W. Edington: *Scripta Met.*, 1981, vol. 15, p. 1043.

42. H. Naziri, R. Pearce, M. Henderson-Brown, and K. Hale: *J. Microsc.*, 1973, vol. 97, p. 229.
43. Y. Kobayashi, Y. Ishida, and M. Kato: *Scripta Met.*, 1977, vol. 11, p. 51.
44. R. Z. Valiev, O. A. Kaibyshev, M. M. Myshlayev, and D. R. Chalaev: *Scripta Met.*, 1980, vol. 14, p. 673.
45. S. H. Reichman and H. W. Smythe: *Int. J. of Powder Met.*, 1970, vol. 6, p. 65.
46. L. M. Moskowitz, R. M. Pelloux, and N. J. Grant: "Proc. 2nd Int. Conf. on Superalloy Processing", MCIC publication MCIC-72-10-Z-1, 1972.
47. J. M. Larson, "Modern Developments in Powder Metallurgy", H. H. Hauser, ed., Plenum Press, New York, NY, 1973, vol. 9, p. 537.
48. R. G. Menzies, J. W. Edington, and G. J. Davies: *Met. Sci. J.*, 1981, vol. 15, p. 210.
49. V. N. Babushkin and A. I. Borisenko: *Zashchita Metall.*, 1968, vol. 4 (3), p. 309.
50. D. F. Kalinovich, I. I. Kovensky, M. D. Smolin, and V. O. Statsenko: *Fiz, Tverd. Tela.*, 1969, vol. 11, p. 2378.
51. C. E. Sessions and T. S. Lundy: *J. Nucl. Mat.*, 1969, vol. 31, p. 316.
52. J. P. A. Immarigeon, G. Van Drunen, and W. Wallace: Proc. 34th Int. Symp. on Superalloys, Claitor's Pub. Div., Baton Rouge, LA.
53. Y. Kobayashi: M. Sc. Thesis, M. I. T., Cambridge, MA, 1974.
54. R. G. Menzies, Ph. D. Thesis, University of Cambridge, England, 1979.
55. R. G. Menzies, J. W. Edington, and G. J. Davies: *Met. Sci. J.*, 1981, vol. 15, p. 217.
56. A. Chaudhari: *J. Inst. Met.*, 1970, vol. 98, p. 114.
57. K. Matsuki and M. J. Yamada: *Jpn. Inst. Met.*, 1973, vol. 37, p. 448.
58. K. Matsuki, Y. Ueno, and M. Yamada: *Jpn. Inst. Met.*, 1974, vol. 38, p. 219.
59. K. Matsuki, Y. Uetani, M. Yamada, and Y. Murakami: *Met Sci. J.*, 1976, vol. 10, p. 235.
60. K. Matsuki, H. Morita, M. Yamada, and Y. Murakami: *Met. Sci. J.*, 1977, vol. 11, p. 156.
61. K. Matsuki, Y. Uetani, M. Yamada, and Y. Murakami: *Met. Sci. J.*, 1976, vol. 10, p. 235.
62. K. Matsuki, K. Minami, M. Tokizawa, and Y. Murakami: *Met. Sci. J.*, 1979, vol. 13, p. 619.
63. K. J. Gardner, P. Griffin, and R. Grimes: "Recrystallization in the Control of Microstructure", the Iron and Steel Institute/The Institute of Metals, London, 1973.
64. M. J. Stowell, B. M. Watts, and D. G. E. Owen: "Recrystallization and the Control of Microstructure", the Iron and Steel Institute/The Institute of Metals, London, 1973.
65. R. Grimes, M. J. Stowell, and B. M. Watts: *Met. Technol.*, 1976, vol. 3, p. 154.
66. B. M. Watts, M. J. Stowell, B. L. Baikie, and D. G. E. Owen: *Met. Sci. J.*, 1976, vol. 10, p. 189.
67. B. M. Watts, M. J. Stowell, B. L. Baikie, and D. G. E. Owen: *Met. Sci. J.*, 1976, vol. 10, p. 198.
68. K. J. Gardner and R. Grimes: *Met. Sci. J.*, 1979, vol. 13, p. 216.
69. R. H. Bricknell and J. W. Edington: *Acta Met.*, 1979, vol. 27, p. 1303.
70. R. J. Roe: *J. Appl. Phys.*, 1965, vol. 36, p. 2024.
71. H. J. Bunge: *Z. Metallk.*, 1965, vol. 56, p. 872.
72. G. J. Davies, D. J. Goodwell, and J. S. Kallend: *J. Appl. Crystallogr.*, 1971, vol. 4, p. 67.
73. J. S. Kallend and G. J. Davies: *Phil. Mag.*, 1972, vol. 25, p. 471.
74. H. Hu: *Texture*, 1974, vol. 1, p. 233.
75. A. H. Clauer, B. A. Wilcox, and J. P. Hirth: *Acta Met.*, 1970, vol. 18, p. 381.
76. J. Washburn and E. R. Parker: *Trans. AIME*, 1952, vol. 194, p. 1076.
77. R. H. Bricknell and J. W. Edington: *Acta Met.*, 1979, vol. 27, p. 1313.
78. R. H. Bricknell and J. W. Edington: *Metall. Trans. A*, 1979, vol. 10A, p. 1257.
79. R. Z. Valiev and O. A. Kaibyshev: *Phys. Stat. Sol.*, 1977, vol. 44A, p. 65.
80. R. Z. Valiev and O. A. Kaibyshev: *Phys. Stat. Sol.*, 1977, vol. 44A, p. 477.
81. R. Z. Valiev, O. A. Kaibyshev, and Sh. Sh. Khannanov: *Phys. Stat. Sol.*, 1979, vol. 52, p. 447.
82. D. Holt: *Trans. TMS-AIME*, 1968, vol. 242, p. 25.
83. P. Chaudhari: *Acta Met.*, 1967, vol. 15, p. 1777.
84. K. Nuttall: *J. Inst. Met.*, 1972, vol. 100, p. 114.
85. A. Arieli, A. K. S. Yu, and A. K. Mukherjee: *Metall. Trans. A*, 1980, vol. 11A, p. 181.
86. R. Kossowski and J. H. Bechtold: *Trans. TMS-AIME*, 1967, vol. 242, p. 716.
87. E. U. Lee and E. E. Underwood: *Metall. Trans.*, 1970, vol. 1, p. 1399.
88. H. Naziri and R. Pearce: *J. Inst. Met.*, 1973, vol. 101, p. 197.
89. R. B. Nicholson: *Electron Microscopy and Structure of Materials*, G. Thomas, ed., Univ. of Calif. Press, Berkeley, CA, 1972, p. 689.
90. R. L. Jones and A. Kelly: *Acta Met.*, 1967, vol. 15, p. 438.
91. R. C. Price and A. Kelly: *Acta Met.*, 1964, vol. 12, p. 159.
92. H. Naziri, R. Pearce, M. Henderson-Brown, and K. F. Hale: *J. Microsc.*, 1973, vol. 97 (1,2), p. 229.
93. R. C. Gifkins: *J. Mat. Sci.*, 1978, vol. 13, p. 1926.
94. K. N. Melton and J. W. Edington: *Metal Sci. J.*, 1973, vol. 7, p. 172.
95. L. C. A. Samuelsson, K. N. Melton, and J. W. Edington: *Acta Met.*, 1976, vol. 24, p. 1017.
96. C. M. Packer, R. H. Johnson, and O. D. Sherby: *Trans. TMS-AIME*, 1968, vol. 242, p. 2485.
97. O. A. Kaibyshev and I. V. Kazachkov: *Fiz. Metal Metalloved*, 1971, vol. 32 (1), p. 205.
98. O. A. Kaibyshev and I. V. Kazachkov: *Fiz. Metal Metalloved*, 1972, vol. 34 (2), p. 396.
99. O. A. Kaibyshev and I. V. Kazachkov: *Soviet Phys. Doklady*, 1973, vol. 17 (7), p. 714.
100. K. N. Melton and J. W. Edington: *J. Inst. Metals*, 1973, vol. 101, p. 122.
101. K. N. Melton, J. W. Edington, J. W. Kallend, and C. P. Cutler: *Acta Met.*, 1974, vol. 22, p. 165.
102. J. S. Kallend and G. J. Davies: *Texture*, 1972, vol. 1, p. 51.
103. K. N. Melton and J. W. Edington: *Scripta Met.*, 1974, vol. 8, p. 1141.